Supplementary Figures Legends.

Supplementary Figure 1. Electron density for capped ligands.

A.   Omit difference electron density for m^{7}GTP contoured at 2.5 σ.

B.   Omit difference electron density for capped RNA in the two independent copies of the bat/H17N10 polymerase complex, contoured at 2.0 σ.

C.   Omit electron density for capped RNA in the influenza B polymerase complex (PDB:5MSG), contoured at 2.0 σ.

D.   Schematic showing 12-mer capped RNA and the 3' and 5' ends of the vRNA promoter used for crystallisation and putative base-pairing between the primer and the template.

Supplementary Figure 2. Capped RNA binding to influenza B/Memphis polymerase.

A.   Close-up of capped RNA binding (blue) to influenza B?memphis polymerase (PDB:5MSG) showing key interacting residues from the cap-binding (orange) and midlink (magenta) domains. The PB1 subunit is in cyan and the helical-lid domain of PB2 is red. To be compared to Figure 1C, the equivalent view for A/H17N10 polymerase.

B.   Table showing equivalence of midlink (magenta) and cap-binding domain (orange) residues between A/Victoria/H3N2, bat A/H17N10 and B/Memphis. Mutation of starred residues in influenza A leads to resistance to VX-787.

Supplementary Figure 3. Kinetics of RNA synthesis by influenza A/H17N10 wildtype and PB2-variant polymerases.

Duplicate RNA synthesis assays were performed as described in the Materials and Methods with 0.25 µM influenza A/H17N10 polymerase, 0.15 µM fluorescently-labelled template RNA, 0.2 mM NTPs and 0.071 (black), 0.143 (red), 0.214 (orange), 0.286 (yellow), 0.429 (light green), 0.714 (dark green), 1.43 (blue) or 4.29 (purple) µM of the capped RNA primer.

(A) and (B) H17N10 wild type influenza polymerase.

(C) and (D) H17N10 PB2 R264A variant influenza polymerase.

(E) and (F) H17N10 PB2 I260A variant influenza polymerase.

(G) and (H) H17N10 PB2 Y432A variant influenza polymerase.

Supplementary Figure 4. Effect of VX-787N on RNA synthesis kinetics.

Duplicate RNA synthesis assays were performed as described in the Materials and Methods with 0.25 µM influenza A/H17N10 polymerase, 0.15 µM fluorescently-labelled template RNA, 0.2 mM NTPs with

(A) and (B) 0 (black), 0.1 (red), 0.25 (orange), 0.5 (yellow), 1 (light green), 5 (dark green), 20 (blue) or 200 (purple) µM of VX-787N

(C) and (D) 0 (black), 0.05 (red), 0.15 (orange), 0.3 (yellow), 1 (light green), 5 (dark green), 20 (blue) or 200 (purple) µM of VX-787N.

(A) and (C) capped RNA (0.5 µM) primed RNA synthesis from the vRNA promoter.

(B) and (D) ApG (0.5 mM) primed RNA synthesis from the vRNA promoter.

Supplementary Figure 5. Comparison of VX-787N and VX-787 binding to influenza A cap-binding domain.

A.   Structural formula for VX-787 (azaindole).

B.   Structural formula for VX-787N (azaindazole).

C.   Omit 2fo-Fc electron density for VX-787N (red) in the A/H5N1 cap-binding domain structure contoured at 1.2 σ.

D.   Hydrogen bond network (green dotted lines) connecting VX-787N to residues in the interior of the cap-binding site (yellow side-chains).

E.   Hydrogen bonds between VX-787 (pink) and residues in the interior of the cap-binding site (cyan side-chains). Drawn from PDB:4P1U.

F.   Comparison of VX-787 and VX-787N by superposition of (D) and (E) via the entire cap-binding domain.

Supplementary Figure 6. Affinity of VX-787N and bat A/H17N10 influenza polymerase.

A.   Structural formula for VX-787N-FAM.

B.   Binding isotherms of bat A/H17N10 polymerase and 0.01 µM fluorescently labelled VX-787N (VX-787N-FAM), were recorded and analysed as described in the Materials and Methods in the absence (black squares and black open circles; duplicate experiments) or presence of 0.001 (red), 0.005 (orange), 0.01 (yellow), 0.05 (light green), 0.1 (dark green), 1 (light blue) or 10 (dark blue) µM VX-787N.

C.   The apparent (microscopic) association constant of polymerase and VX-787N-FAM derived from (A) decreases with increasing competitor VX-787N. Fitting to the quadratic velocity equation yields the apparent inhibition constant Ki app (VX-787N) = 0.035 ±0.008 µM (error of the fitting routine), which translates into the true inhibition constant Ki (polymerase + VX-787N) ~ 0.013 µM (competitive inhibition; K_D (polymerase VX-787N-FAM) ~ 0.006 µM. (See Materials and Methods).

Supplementary Figure 7. Comparison of VX-787N binding to influenza A and B cap-midlink double domains.

A. Omit difference electron density for VX-787N in the A/Victoria/H3N2 structure contoured at 2.5 σ.

B. Omit difference electron density for VX-787N in the B/Memphis structure, contoured at 2.0 σ.

C. Comparison of the structures of VX-787N bound to A/Victoria/H3N2 (dark colours) and B/Memphis (light colours) cap-midlink double domains after superposition via the cap-binding domains. Note that the midlink domain is shifted between the two structures. The substitution in influenza B of Gln325 instead of Phe323 eliminates the pi-stacking with the compound and leaves a void in the structure. Other interacting residues from the cap-binding domain are omitted for clarity (see Figures 6B,D). Equivalent residues in influenza A and B are listed underneath.

D. The A/Victoria/H3N2 cap-binding domain with bound VX-787N (cyan) is superposed on the cap-binding domain with bound capped RNA (blue) in the 'priming' conformation. Ser324 does not make direct contact with the inhibitor. Gln306 can make hydrogen bonds to the ribose of the capped RNA but would clash with VX-787N.

Supp. Figure 1

A

m⁷GTP

B

m⁷G

A1

A2

U3

C

D
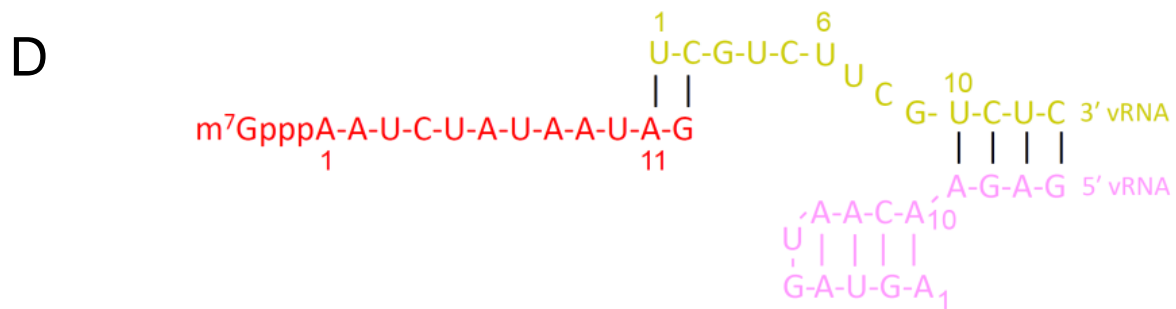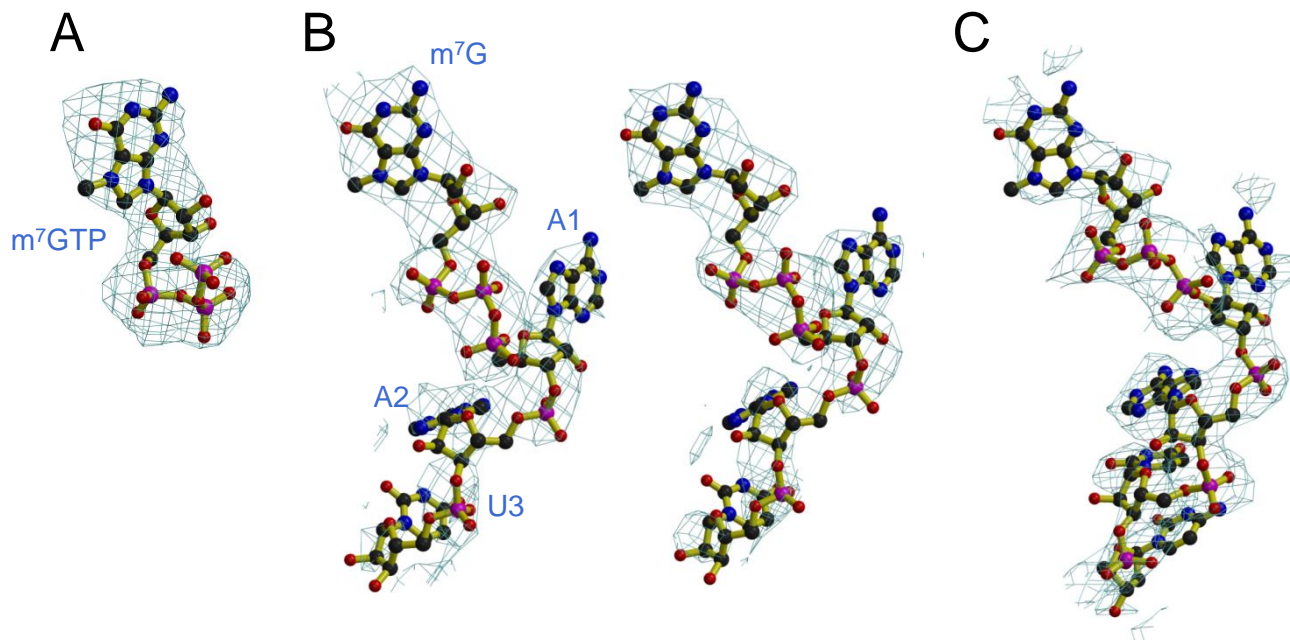
Supp. Figure 2

A
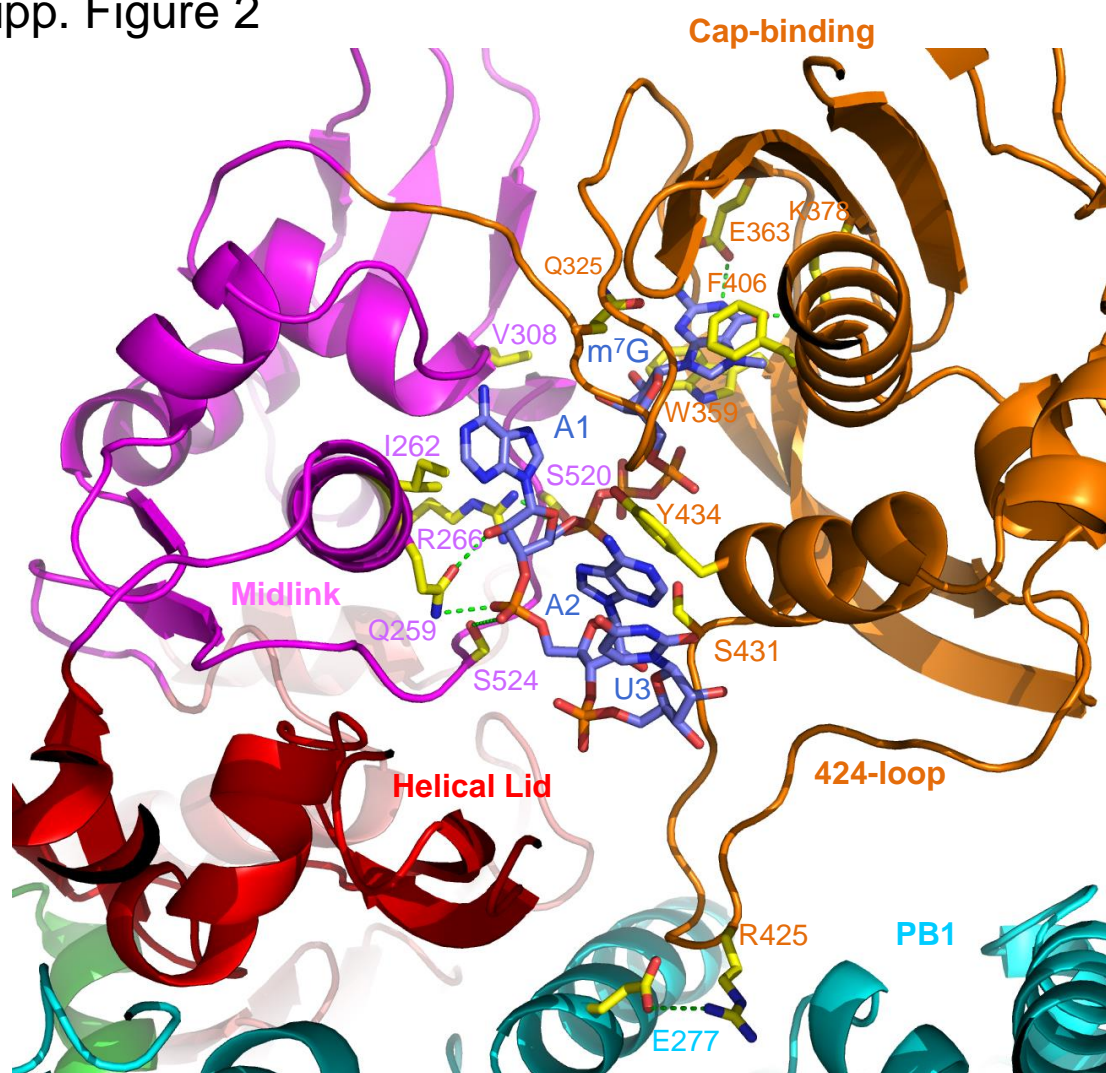
B

A/H3N2	A/H17N10	B/Memphis
Q257	Q257	Q259
I260	I260	I262
R264	R264	R266
Q306*	Q306	V308
F323	F323	Q325
S324*	S324	R326
H357	F357	W359
E361	E361	E363
K376	K376	K378
F404	F404	F406
R423	R423	R425
N429	N429	S431
H434	Y434	Y434
N510*	N510	E511
S519	S519	S520
G523	G523	S524

Supp. Figure 3
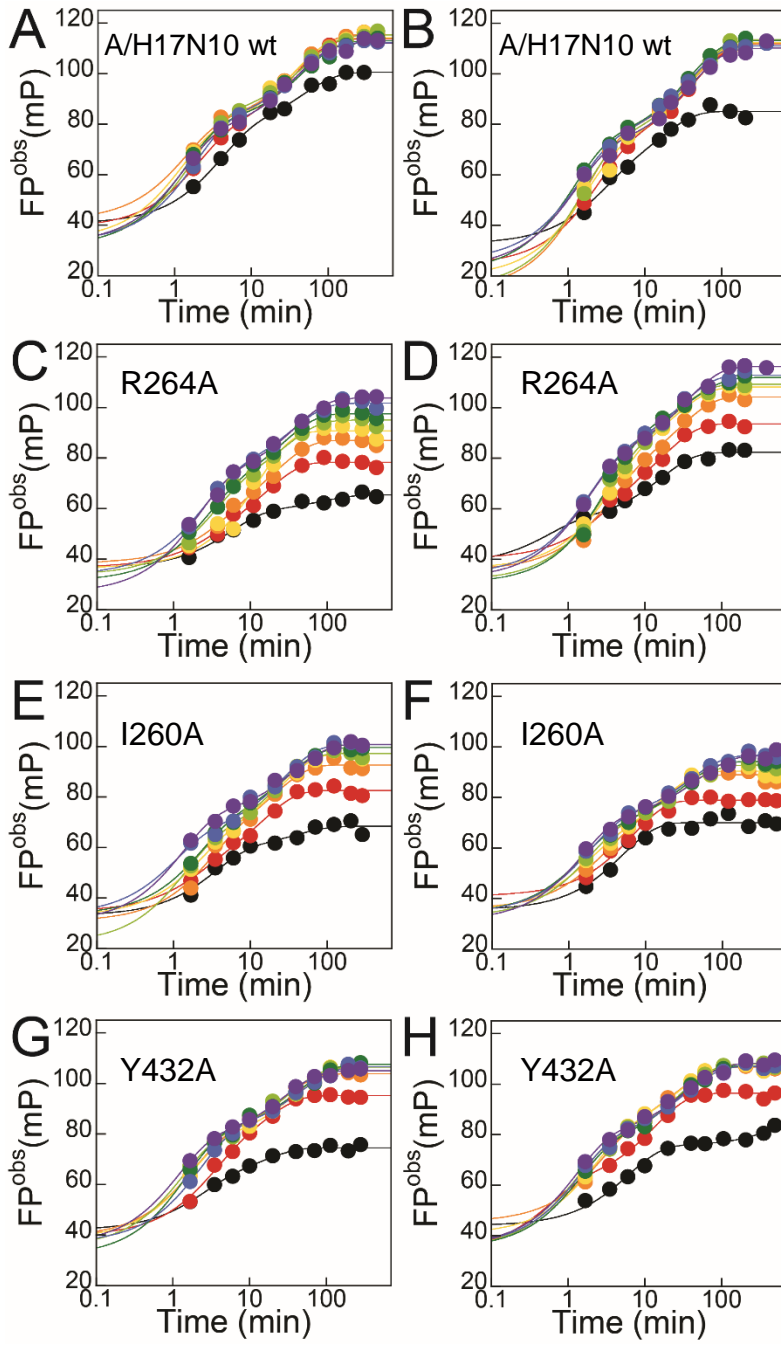
Supp. Figure 4

Supp. Figure 5

A   VX-787

B   VX-787N

C

D   Ser320   Arg332   Glu361   Water   Lys376   VX-787N

E   Arg332   Glu361   Lys376   VX-787 (PDB:4P1U)

F   Ser320   Arg332   Glu361   Lys376

Supp. Figure 6.

A

VX-787N-FAM

B

C
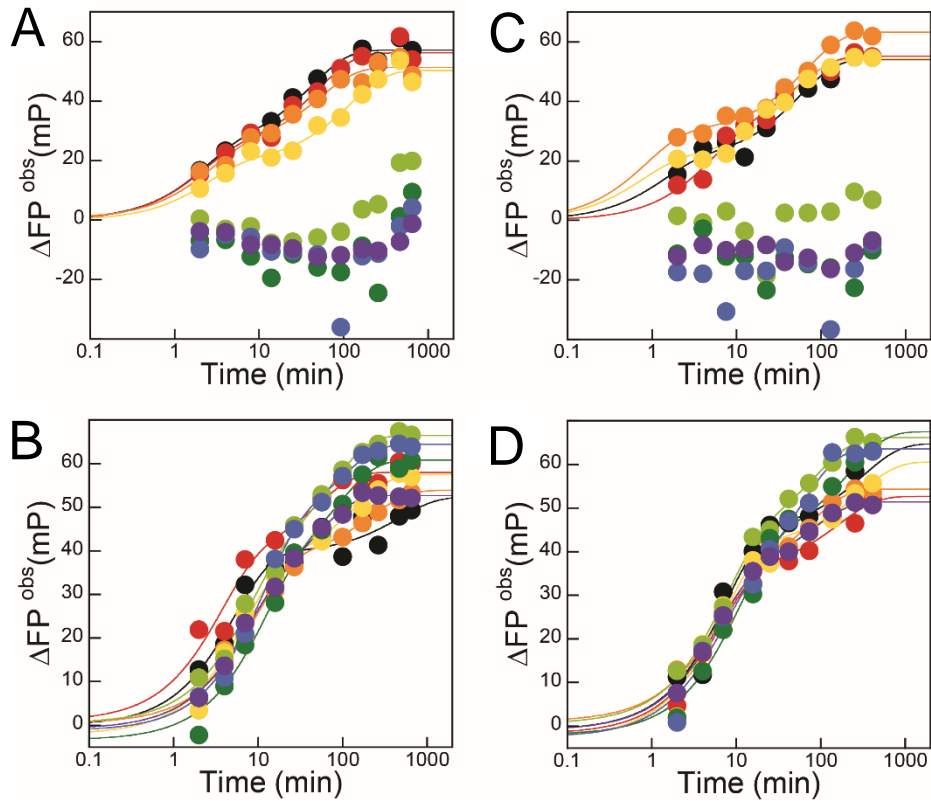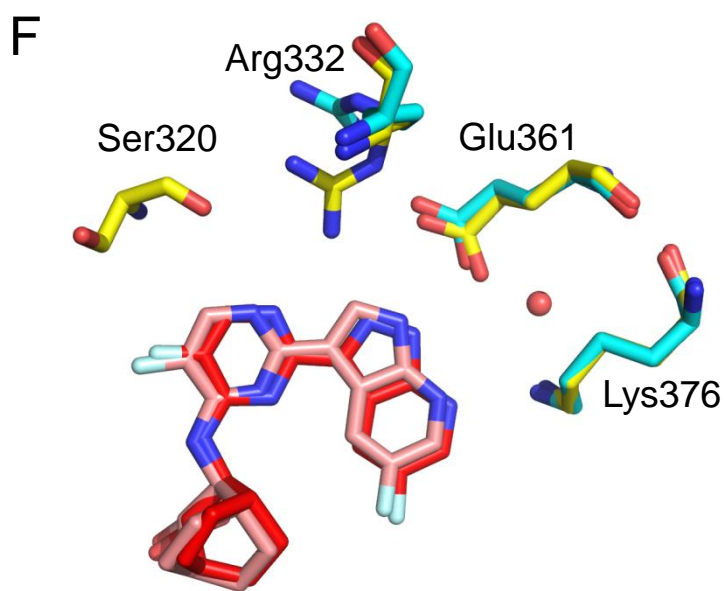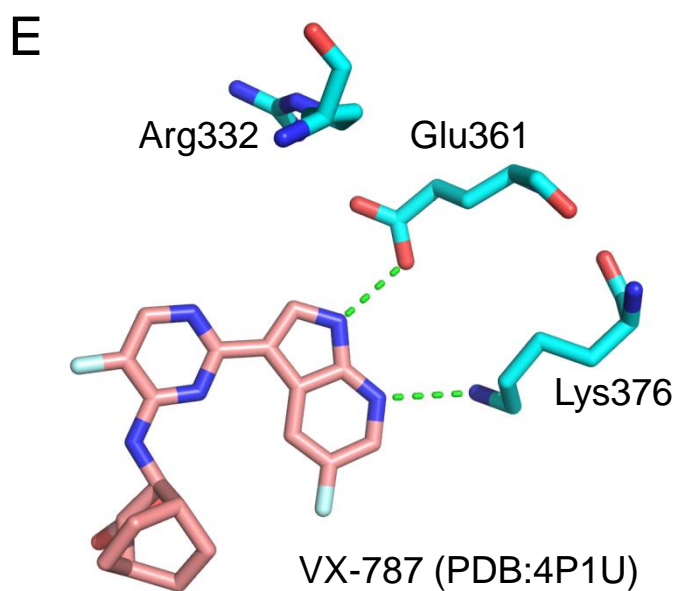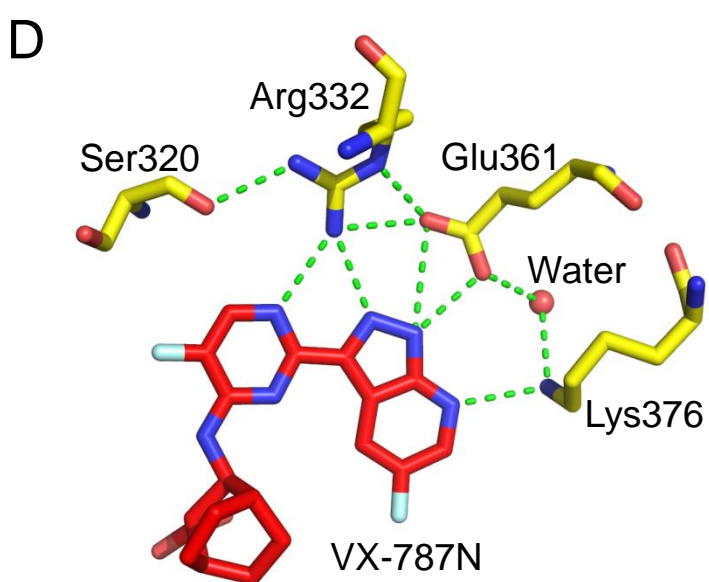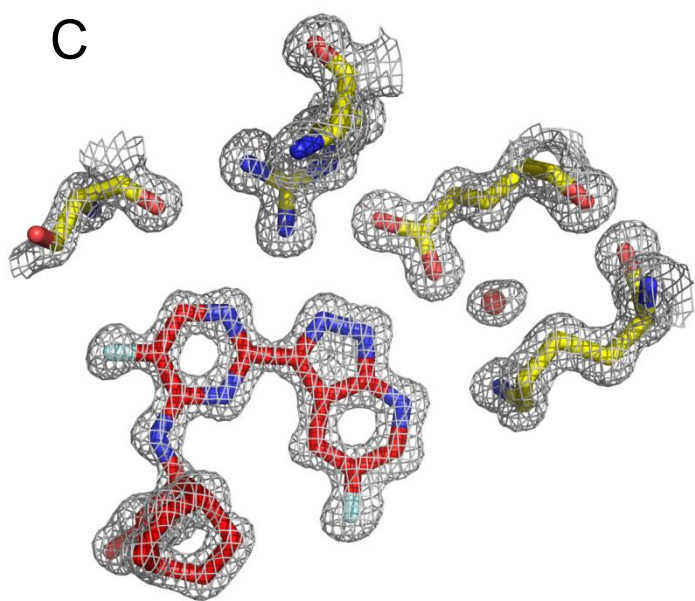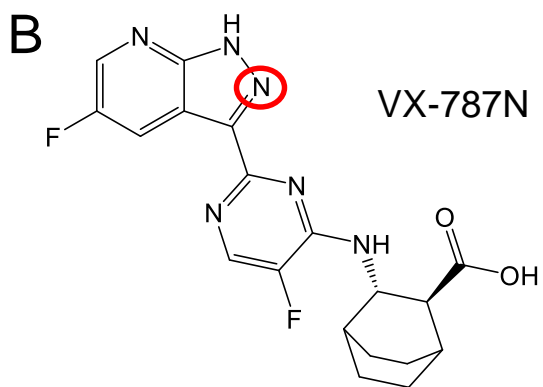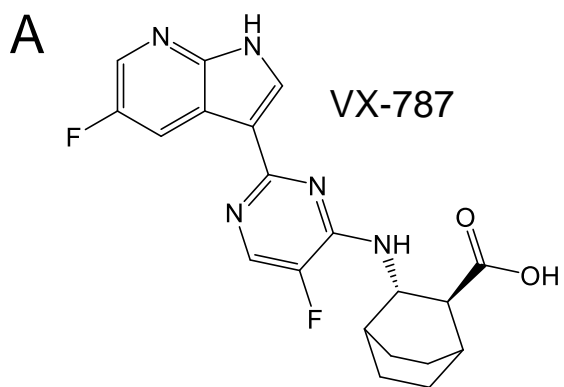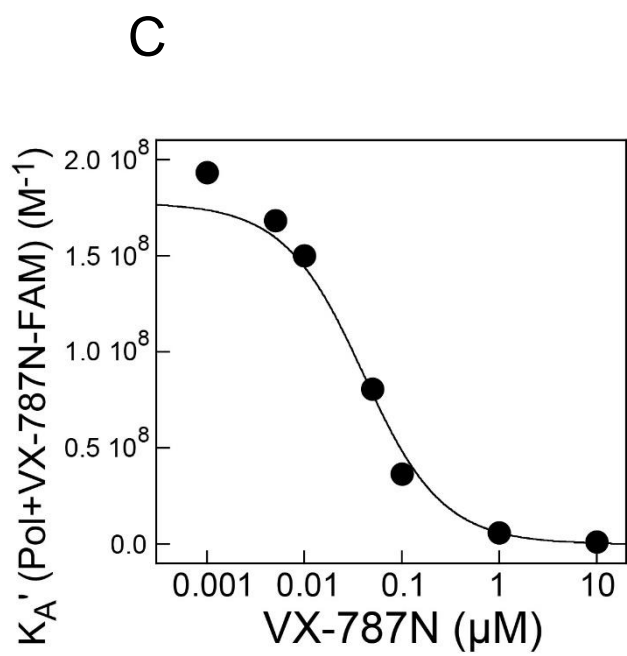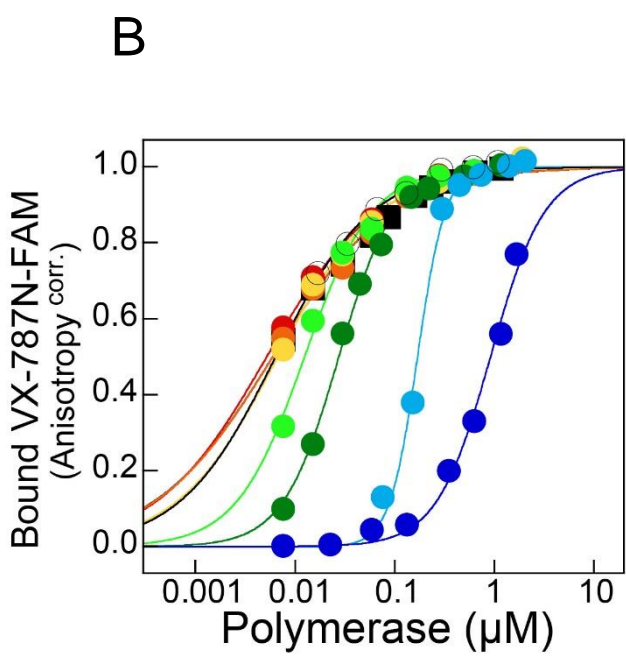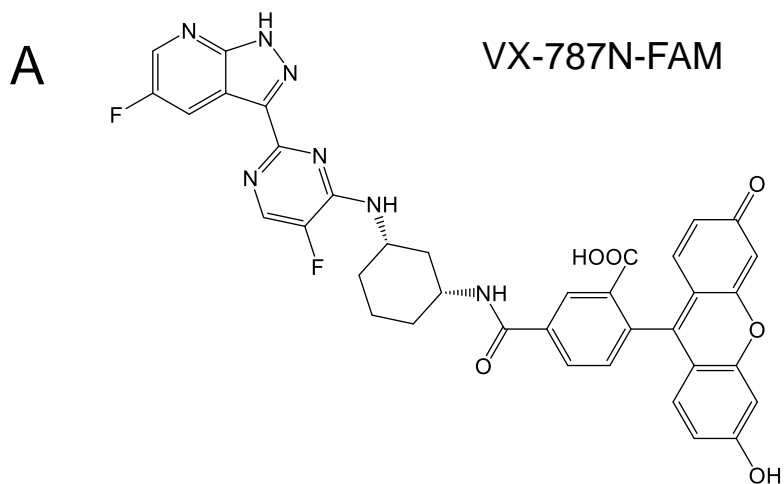
Supp. Figure 7

A
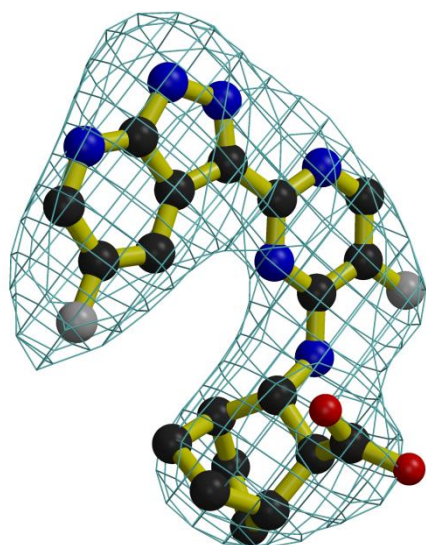
B
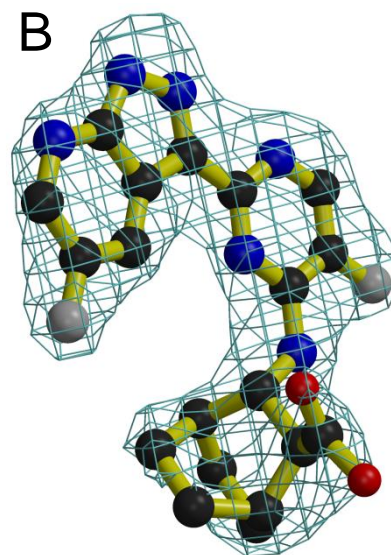
C
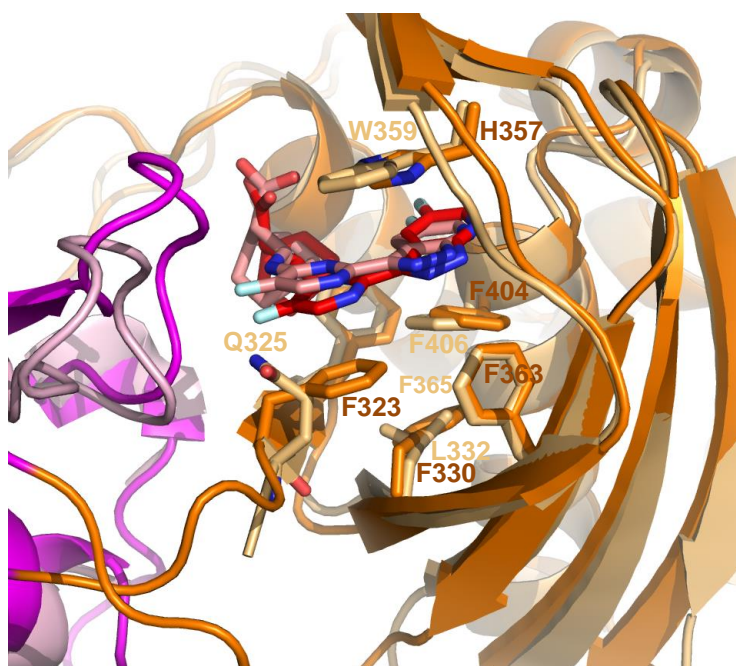
A/H3N2 cap-midlink VX-787N (dark colours)

B/Memphis cap-midlink VX-787N (light colours)
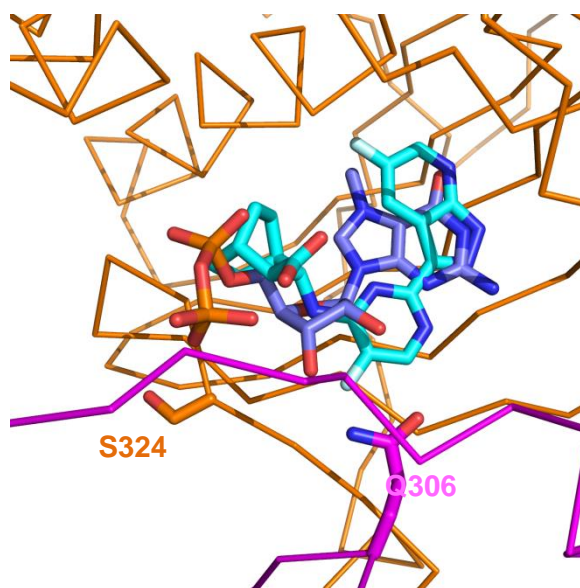
A/H3N2	B/Memphis
F323	Q325
F330	L332
H357	W359
F363	F365
F404	F406

D

VX-787N
Capped RNA

Supplementary Table 1. Additional Crystallographic data processing and refinement statistics.

Crystal	A/H5N1 cap-binding domain +VX-787N	A/Victoria/H3N2 PB2 cap-midlink double-domain +VX-787
Diffraction Data		
Space group	$P6_1$	$P1$
Cell dimensions (Å)	a=62.49 b=62.49 c=69.97	a=54.49 b=80.32 c=92.32 α=89.54 β=107.12 γ=99.11
Wavelength (Å)	1.0615	0.966
Beamline	ID23-1	ID30A1
Resolution range of data (last shell) (Å)	50-1.00 (1.06-1.00)	50-2.70 (2.77-2.70)
Completeness (last shell) (%)	94.0 (70.8)	94.8 (94.2)
R-sym (last shell)	0.065 (0.508)	0.091 (0.698)
I/σI (last shell)	12.61 (1.46)	5.99 (1.02)
CC(1/2)	0.996 (0.846)	0.991 (0.508)
Redundancy (last shell)	4.46 (2.04)	1.69 (1.55)
Refinement		
Reflections in refinement: work (free)	74557 (3907)	36631 (1837)
R-work (last shell)	0.139 (0.388)	0.243 (0.359)
R-free (last shell)	0.164 (0.383)	0.281 (0.381)
No of non-hydrogen atoms	1537	9091
Protein	1345 (1 molecule)	8753 (4 molecules)
Ligand	29	116
Solvent	163	222
Geometry and B-factors		
RMS(bonds)	0.010	0.010
RMS(angles)	1.587	1.496
Ramachandran favoured (%)	99.34	96.63
Ramachandran outliers (%)	0	0.18
Molprobity score	1.47	1.82
Clash score	3.56	3.02
Average B-factor (Å^2)		
All atoms	20.6	50.8
Protein	18.9	51.2
Ligand	17.5	31.6
Solvent	34.5	30.3